A Fault Ride-Through Strategy for Grid-Forming Converters Under Symmetrical and Asymmetrical Grid Faults

Xianxian Zhao[a], Xavier Kestelyn[b], Damian Flynn[a]
[a] School of Electrical and Electronic Engineering, University College Dublin, Dublin, Ireland
[b] ULR 2697–L2EP, Centrale Lille, Junia ISEN Lille, Arts et Metiers Institute of Technology, University of Lille, Lille, France
xianxian.zhao@ucd.ie, xavier.kestelyn@ensam.eu, damian.flynn@ucd.ie

***Abstract*—In order to maintain grid-forming converter (GFM) voltage source behavior under current limiting mode, a threshold virtual impedance (TVI) current limiting control is proposed, which is controlled in the positive and negative sequence synchronous reference frames for symmetrical and asymmetrical fault conditions. The converter current is strictly limited within the maximum limit without the need for current saturation limiters. Since the TVI control is based on 3-phase sinusoidal currents, it is shown that using the measured current instead of the existing current reference for the TVI control may cause oscillatory behaviour when a large switching delay is considered. Since sequence extraction control is necessary, the paper also compares GFM dynamic stability under the three well-known sequence extraction methods (i.e. delay cancellation, dual second order generalized integrator, and decoupled double synchronous reference frame). It is shown that the differences are small when GFM is not in current limiting mode, but they are large when GFM is in current limiting mode or switching delays are considered.**

***Index Terms*—Asymmetrical grid fault, sequence extraction, threshold virtual impedance current limiting, fault ride-through (FRT), grid-forming converter (GFM).**

I. INTRODUCTION

Present power grids are mostly powered by synchronous generators that created point of connections, to which voltage and frequency are maintained in acceptable limits, to supply different kind of loads. With the growing part of grid-following converters (GFLs), that use the points of connections to inject power to the grid in a synchronized way [1], the power system becomes less and less "stiff", i.e. be able to maintain the expected voltage and frequency levels at the connection points [2][3]. Grid-forming converters (GFMs) propose to mimic synchronous generators by creating their own voltage and frequency and provide a way to response to voltage and frequency disturbances. Their capabilities leads to the idea of 100% power electronics grids since GFMs are seen as a replacement for synchronous generators in future power grids [4][5].

A main difference between GFMs and synchronous generators comes from their behaviour when faults occur. Since mimicking the overcurrent capability of synchronous generators would necessitate an oversizing of power converters that will lead to unacceptable over costs, current limiting controls must be added to protect the converters in case of faults. These necessary controls have a great impact on GFM controllability and hence the overall transient stability of power grids with a high penetration of GFMs.

GFMs without current limitations could tightly control the grid voltage, with reduced concern over system transient stability for large disturbances, assuming robust small-signal stability. However, as voltage source converters have much lower overcurrent ability when compared to synchronous generators [6], current limiting control is necessary to protect the converters, which greatly impacts on GFM controllability, and, hence, transient stability. Current limiting control techniques for GFMs can be categorised as current reference saturation, virtual impedance, and a combination of both. Saturation techniques can strictly limit the GFM current, but the outer voltage control loop becomes inactive, and anti-windup techniques must be implemented for the PI outer voltage control loop [7][8]. In contrast, threshold virtual impedance (TVI) current limiting avoids the above disadvantages by emulating the effect of incorporating an impedance when the converter current exceeds a defined value, such that GFM voltage source behaviour is retained, but behind an impedance [9].

The TVI current limiting design for GFMs under balanced faults is well-known [9], and the transient stability of GFMs under such current limiting control has been extensively studied [10]-[13]. However, for unbalanced fault conditions, TVI current limiting control cannot be used directly, and GFM transient stability is unclear, since additional sequence extraction control should be added, either for the current limiting control (e.g. avoiding distorted current waveforms [14]) or for GFM overall control (e.g. suppressing negative voltage during asymmetrical faults [16]).

The traditional TVI control is not suitable for GFMs for unbalanced situations since the current amplitude (calculated in the $\alpha\beta$ static or dq synchronous reference frame) for triggering TVI control and generating the virtual impedance is no longer a constant, but, instead, a constant with a superimposed sine wave of twice the fundamental frequency. If this oscillating current is directly used, the virtual voltage drop and hence the voltage references will oscillate, causing unacceptable GFM performance for unbalanced conditions. Hence, a new TVI current limiting control is proposed in [14][15] for GFM under unbalanced situations, where the current amplitude is based on the three-phase current amplitude. However, an issue with this method is that TVI control is only activated when the current saturation limiters are active, such that the GFM voltage source characteristics are not preserved. In fact, this TVI current limiting control can be viewed as an anti-windup technique for the outer voltage PI controller. In [16], another TVI current limiting control is proposed, based on the measured output voltage difference (instead of the converter current) to trigger the TVI control and generate the virtual impedance. However, the current saturation limiters must be activated, otherwise, the output voltage difference and virtual impedance will be zero.

GFM dynamic stability under different sequence extraction methods also needs to be assessed, as existing research on GFMs does not clearly justify the choice of one method over another. In addition, how the various sequence extraction methods affect control performance requires more detailed study.

The main contributions of the paper are:

- A TVI current limiting control for GFM fault-ride through symmetrical and asymmetrical faults is designed, where "hard" current saturation limiters are not needed and GFM voltage source characteristics are preserved;
- GFM dynamic performance is compared when using the measured phase current and phase current reference for triggering TVI control, with the switching delay also considered, since, normally, the measured current is used;
- Since each sequence extraction method creates a certain delay, and distinct functionalities which affect overall GFM behaviour differently, GFM dynamic stability is compared for the three well-known sequence extraction methods, by considering whether the GFM is in current limiting mode or not, and considering the switching delay impact, i.e. delay cancellation, decoupled double synchronous reference frame, and dual second order generalised integrator.

The remainder of the paper is organised as follows. Section II presents an overview of the proposed GFM control in double sequence synchronous reference frame. In Section III, the proposed TVI current limiting control for GFMs is presented. In Section IV, three sequence extraction methods are introduced, and their performance is compared under ideal voltage source situations. In Section V, simulation cases are studied to compare the proposed TVI current limiting control and existing approaches [14][15], and to assess GFM dynamics under the different sequence extraction methods. Finally, conclusions and future work are given in Section VI.

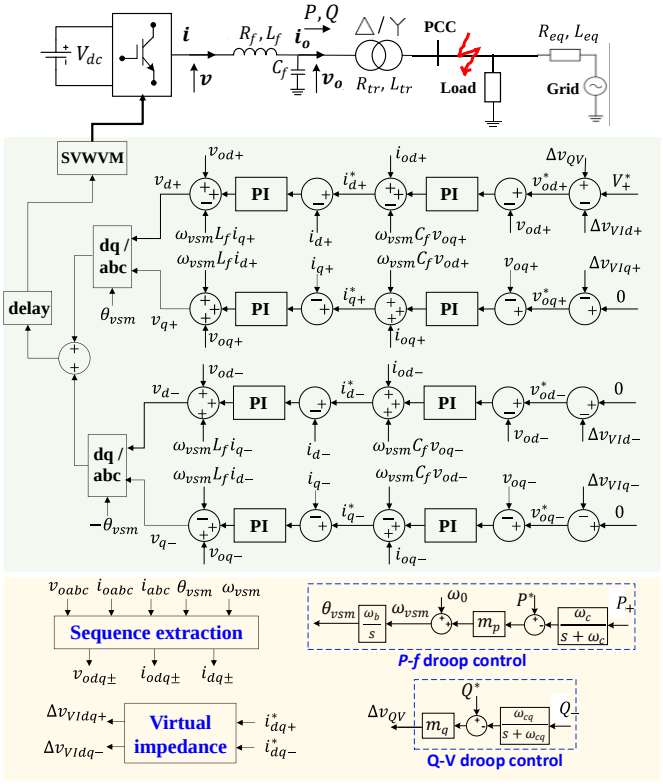

Figure 1. Power circuit schematic and control model of a GFM operating in both positive- and negative-sequence synchronous reference frames.

II. GFM Controlled in Double Sequence Synchronous Reference Frames

Fig. 1 shows a grid-forming converter connected to a load and equivalent grid through a Δ-Yg transformer. R_f, L_f and C_f are resistance, inductance and capacitance of the LC filter. R_{tr} and L_{tr} are the Δ-Yg transformer resistance and inductance. R_{eq} and L_{eq} are equivalent grid resistance and inductance. Note that the Δ feeder connection prevents zero sequence currents at the point of common coupling (PCC), and, hence, only positive and negative sequence fault currents are of interest.

P/f droop control is implemented to achieve power-angle synchronisation, but it is noted that alternative control techniques can be applied, e.g. virtual synchronous generator, virtual oscillator. Cascaded voltage and current proportional integral (PI) control, with d- and q-axis decoupling and feedforward compensation, is implemented in both the positive and negative sequence synchronous reference frame. Using the synchronous reference frame provides the inherent benefit of independent control of the positive and negative sequence output voltage. The converter voltage references generated from the two control loops are then transformed into the static abc reference frame using two inverse Park

transformations, $P^{-1}(\theta_{vsm})$ and $P^{-1}(-\theta_{vsm})$, before being added, delayed, and finally sent to the pulse width modulator (PWM) unit. The delay module mimics the switching delay. The orientation of the dq coordinate is defined as d-axis being aligned with a phase and q-axis leading 90 degrees.

In order to protect the GFM from overcurrents, current limiting control must be implemented. The proposed TVI current limiting control will be described in Section III, but sequence extraction control is needed to obtain the positive and negative voltage and current signals. Three sequence extraction methods will be detailed in Section IV.

III. Proposed TVI Current Limiting Control for GFMs Under Symmetrical and Asymmetrical Faults

A. Description of The Proposed TVI Control

As the instantaneous sum of the two contrarotating vectors $\boldsymbol{i}^*_{dq+}$ and $\boldsymbol{i}^*_{dq-}$ results in an elliptical trajectory of the total current reference vector (i.e. the rms current oscillates at twice the grid fundamental frequency) under asymmetrical faults or voltage dips, the proposed TVI current limiting control is triggered based on the amplitude of the three-phase current reference in the static reference frame. The virtual resistance and reactance are generated according to (1) and (2).

$$R_{VI} = k_{pVI} * \max\left(0, I_p^* - I_{nom}\right), \tag{1}$$

$$X_{VI} = \sigma_{X/R} R_{VI}. \tag{2}$$

where k_{pVI} is virtual resistance gain proportional to the exceeded current of $\max\left(0, I_p^* - I_{nom}\right)$, $\sigma_{X/R}$ is the virtual reactance and resistance ratio, and I_p^* is the maximum value across the amplitude of the three-phase current references, I_a^*, I_b^*, and I_c^*, which is

$$I_p^* = \max\{I_a^*, I_b^*, I_c^*\}, \tag{3}$$

$$\begin{aligned}
I_a^* &= \| \boldsymbol{i}^*_{dq+} \|^2 + \| \boldsymbol{i}^*_{dq-} \|^2 + 2 \| \boldsymbol{i}^*_{dq+} \| \| \boldsymbol{i}^*_{dq-} \| \cos(\varphi), \\
I_b^* &= \| \boldsymbol{i}^*_{dq+} \|^2 + \| \boldsymbol{i}^*_{dq-} \|^2 + 2 \| \boldsymbol{i}^*_{dq+} \| \| \boldsymbol{i}^*_{dq-} \| \cos\left(\varphi - \tfrac{2\pi}{3}\right), \\
I_c^* &= \| \boldsymbol{i}^*_{dq+} \|^2 + \| \boldsymbol{i}^*_{dq-} \|^2 + 2 \| \boldsymbol{i}^*_{dq+} \| \| \boldsymbol{i}^*_{dq-} \| \cos\left(\varphi + \tfrac{2\pi}{3}\right),
\end{aligned} \tag{4}$$

where, $\|\cdot\|^2$ denotes the square norm, and $\boldsymbol{i}^*_{dq+} = i^*_{d+} + j i^*_{q+}$ and $\boldsymbol{i}^*_{dq-} = i^*_{d-} + j i^*_{q-}$ denote the positive and negative sequence current reference from the outer voltage PI control block, $\varphi = \theta^*_- - \theta^*_+$ indicates the angle difference, with θ^*_+ and θ^*_- given by

$$\begin{aligned}
\theta^*_+ &= \tan^{-1}\left(i^*_{q+}/i^*_{d+}\right), \\
\theta^*_- &= -\tan^{-1}\left(i^*_{q-}/i^*_{d-}\right).
\end{aligned} \tag{5}$$

Based on R_{VI} and X_{VI}, the virtual positive and negative sequence voltage drops are given by

$$\begin{bmatrix} \Delta v_{VId+} \\ \Delta v_{VIq+} \end{bmatrix} = \begin{bmatrix} R_{VI} & -X_{VI} \\ X_{VI} & R_{VI} \end{bmatrix} \begin{bmatrix} i^*_{d+} \\ i^*_{q+} \end{bmatrix}, \tag{6}$$

$$\begin{bmatrix} \Delta v_{VId-} \\ \Delta v_{VIq-} \end{bmatrix} = \begin{bmatrix} R_{VI} & X_{VI} \\ -X_{VI} & R_{VI} \end{bmatrix} \begin{bmatrix} i^*_{d-} \\ i^*_{q-} \end{bmatrix}, \tag{7}$$

The description of the proposed TVI control is thus completed. Two important issues should be noted here:

- In (1), $I_{nom} < I_{max}$, where I_{max} is the maximum converter current allowed to avoid converter damage. Therefore, the proposed TVI control is activated before I_p^* reaches I_{max}, and aims to limit $I_p^* \le I_{max}$ by suitably designing the gains k_{pVI} and $\sigma_{X/R}$. Current saturation limiters at the output of the current PI control block are not required. Hence, GFM voltage source behaviour is preserved when in current limiting mode. The existing TVI control in [14][15], however, is activated only when the current saturation limiters are active, and, hence, GFM voltage source behaviour is not fully preserved, such that stability analysis becomes more challenging. Moreover, since the integrator of the voltage PI control block is still integrating when the current saturation limiters are active, the post-fault voltage will be higher than the reference value, and take a long time to recover (demonstrated later in Section V).
- In (1), I_p^* cannot be replaced by I_p, where I_p is calculated based on the measured real-time sequence current using the same procedure as (3)(4). The logic here is that while I_p^* can be directly obtained from the double sequence voltage control blocks, to obtain I_p, sequence extraction is required to obtain the positive and negative current signals when calculating (3) and (4). Since sequence extraction unavoidably introduces delays, which may cause the GFM output to oscillate and even become unstable for severe faults, it follows that GFM controllability and damping capability is reduced.

B. Calculation of The TVI Gains

Similar to [9][10], the principle of the proposed TVI control is to limit the converter steady-state phase current to I_{max} when a bolted fault is applied at the PCC. Based on this principle and (1)(2), it follows that

$$\frac{V_{ref}}{I_{max}} = \sqrt{\left(R_{VI}^{max} + R_g\right)^2 + \left(\sigma_{X/R} R_{VI}^{max} + X_g\right)^2}, \tag{8}$$

$$R_{VI}^{max} = k_{pVI}(I_{max} - I_{nom}). \tag{9}$$

Based on (8) and (9), k_{pVI} can be obtained, as $\sigma_{X/R}$ is usually prescribed according to damping and stability requirements.

Note that no negative or positive sequence current limiting priority is implemented, but the negative or positive sequence current references are dynamically scaled down according to their phase amplitude and the virtual impedance gains. The resulting benefit is that current capacity utilisation can always be maximised, without distinguishing fault types. So, for example, assume that negative sequence current is prioritised. To obtain the positive and negative gains k_{pVI+} and k_{pVI-}, a worst case unbalanced situation (i.e. largest negative sequence

PCC voltage occurs) needs to be considered, i.e. the worst case negative sequence voltage will be suppressed by the GFM by using the permitted negative sequence current capacity, while the permitted positive sequence current capacity will be used to support the positive sequence voltage. Based on this priority design, a fraction of the current capacity should be allocated for negative sequence voltage suppression. If a balanced fault now occurs (such that negative sequence voltage doesn't apply), the GFM cannot use all its current capacity to support the grid voltage, since part of the capacity is reserved for negative sequence voltage suppression, which is clearly wasteful. A possible solution here is to switch the positive sequence gain k_{pVI+} to a different value.

Regarding the choice of $\sigma_{X/R}$, the value chosen should be much smaller than that for a GFM only assuming symmetrical faults. Since a smaller $\sigma_{X/R}$ can increase GFM damping capability [12], two main factors should be recognised: (1) sequence extraction is required for either GFM current limiting or overall GFM control, and, as illustrated above, sequence extraction unavoidably introduces delays, which requires greater damping capability; and (2) the current reference, I_p^*, instead of the real-time current is used for the virtual impedance calculation, such that the natural filtering effect on the real-time current is not applicable to I_p^*.

IV. Sequence Extraction for GFMs

Three sequence extraction methods, i.e. quarter cycle delay cancellation, dual second order generalised integrator (DSOGI), and decoupled double synchronous reference frame (DDSRF) are described here. Notch filter based sequence extraction is also described here for completeness as some papers are using it. The performance of the three methods is then compared, assuming an ideal unbalanced voltage source. In the following, only current signals, instead of both current and voltage signals, are used when describing the individual methods.

Without a zero sequence component, the 3-phase current signals in the stationary $\alpha\beta$ reference frame can be expressed by the positive and negative sequence components as follows

$$\boldsymbol{i}_{\alpha\beta} = \boldsymbol{i}_{\alpha\beta+} + \boldsymbol{i}_{\alpha\beta-} = \boldsymbol{i}_{dq+}e^{j\omega t} + \boldsymbol{i}_{dq-}e^{-j\omega t}, \quad (10)$$

where, $\boldsymbol{i}_{\alpha\beta} = i_\alpha + ji_\beta$, $\boldsymbol{i}_{\alpha\beta+} = i_{\alpha+} + ji_{\beta+}$ and $\boldsymbol{i}_{\alpha\beta-} = i_{\alpha-} + ji_{\beta-}$ are the positive and negative sequence current vectors in the $\alpha\beta$ plane, respectively, while $\boldsymbol{i}_{dq+} = i_{d+} + ji_{q+}$ and $\boldsymbol{i}_{dq-} = i_{d-} + ji_{q-}$ are the positive and negative sequence current vectors in the dq plane rotating at ωt and $-\omega t$, respectively.

Implementing two Park transformations, $P(\theta)$ and $P(-\theta)$, i.e. multiplying (10) by $e^{-j\omega t}$ and $e^{j\omega t}$, where $\theta = \omega t$, (10) can be expressed as (11) and (12), respectively.

$$\boldsymbol{i}_{\alpha\beta}e^{-j\omega t} = \boldsymbol{i}_{dq+} + \boldsymbol{i}_{dq-}e^{-j2\omega t}, \quad (11)$$

$$\boldsymbol{i}_{\alpha\beta}e^{j\omega t} = \boldsymbol{i}_{dq+}e^{j2\omega t} + \boldsymbol{i}_{dq-}. \quad (12)$$

In (11)(12) it is seen that $\boldsymbol{i}_{dq+}$ and $\boldsymbol{i}_{dq-}$ are coupled. To remove this coupling effect, a sequence extraction is required, with four such methods described in the following.

A. Quarter Cycle Delay Cancellation Using Fortescue Matrix

Fig. 2 shows the delay cancellation sequence extraction method, based on the Fortescue matrix implementation. When applying the Clark transformation, Fortescue's symmetrical components method and Clark inverse transformation [17][18], the instantaneous positive sequence current based on the $\alpha\beta$ reference frame $\boldsymbol{i}_{\alpha\beta+}$ can be calculated as

$$\boldsymbol{i}_{\alpha\beta+} = [T_{\alpha\beta}]\boldsymbol{i}_{abc+} = [T_{\alpha\beta}][T_+]\boldsymbol{i}_{abc} = [T_{\alpha\beta}][T_+][T_{\alpha\beta}]^{-1}\boldsymbol{i}_{\alpha\beta} = \frac{1}{2}\begin{bmatrix} 1 & -e^{-j\pi/2} \\ e^{-j\pi/2} & 1 \end{bmatrix}\boldsymbol{i}_{\alpha\beta}, \quad (13)$$

where $[T_{\alpha\beta}] = \frac{2}{3}\begin{bmatrix} 1 & -\frac{1}{2} & \frac{1}{2} \\ 0 & \frac{\sqrt{3}}{2} & -\frac{\sqrt{3}}{2} \end{bmatrix}$, $[T_+] = \frac{1}{3}\begin{bmatrix} 1 & a^2 & a \\ a & 1 & a^2 \\ a^2 & a & 1 \end{bmatrix}$, $a = e^{-j2\pi/3}$, and $e^{-j\pi/2}$ is a phase-shift operator in the time-domain associated with a quarter cycle delay, $T_b/4$, waveform of the original in-phase waveform, where T_b represents the fundamental period.

Similarly, the instantaneous negative sequence current based on the $\alpha\beta$ reference frame $\boldsymbol{i}_{\alpha\beta-}$ can be obtained as

$$\boldsymbol{i}_{\alpha\beta-} = \frac{1}{2}\begin{bmatrix} 1 & e^{-j\pi/2} \\ -e^{-j\pi/2} & 1 \end{bmatrix}\boldsymbol{i}_{\alpha\beta}. \quad (14)$$

To be clear, (13)(14) can be combined into matrix form as

$$\begin{bmatrix} i_{\alpha+} \\ i_{\beta+} \\ i_{\alpha-} \\ i_{\beta-} \end{bmatrix} = \frac{1}{2}\begin{bmatrix} 1 & 0 & 0 & -1 \\ 0 & 1 & 1 & 0 \\ 1 & 0 & 0 & 1 \\ 0 & 1 & -1 & 0 \end{bmatrix}\begin{bmatrix} i_\alpha \\ i_\beta \\ i_{\alpha\perp} \\ i_{\beta\perp} \end{bmatrix}, \quad (15)$$

where, $i_{\alpha\perp}$ and $i_{\beta\perp}$ are $T_b/4$ delayed i_α and i_β, respectively.

The positive and negative sequence current in the dq reference frame $\boldsymbol{i}_{dq+}$ and $\boldsymbol{i}_{dq-}$ are then obtained by implementing two Park transformations, $P(\theta_{vsm})$ and $P(-\theta_{vsm})$, to $\boldsymbol{i}_{\alpha\beta+}$ and $\boldsymbol{i}_{\alpha\beta-}$. Here θ_{vsm} is used, since the GFM double sequence voltage and current control are based on the synchronous reference frame rotating at θ_{vsm} and $-\theta_{vsm}$ speed.

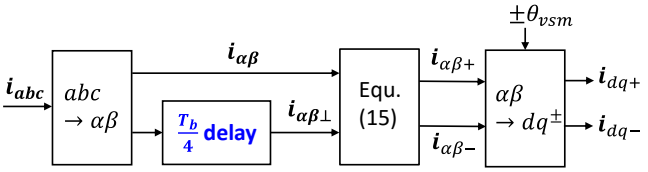

Figure 2. Sequence extraction using quarter cycle delay cancellation.

B. Dual Second Order Generalised Integrator (DSOGI)

The dual second order generalised integrator sequence extraction in [19] is adapted for GFMs, and shown in Fig. 3. It agrees with the delay cancellation method, except that the variables i_α, i_β, $e^{-j\pi/2}i_\alpha$ and $e^{-j\pi/2}i_\beta$ are obtained from two second order generalised integrator (SOGI), as shown in Fig.

4. One of the main features of the SOGI is its dual outputs, i.e. the band-pass filtered signal x' and a 90° shifted orthogonal low-pass filtered signal $x'_\perp = e^{-j\pi/2}x'$. In Fig. 3, following [19], $k_{sogi} = \sqrt{2}$ is chosen, which provides a good tradeoff between stabilisation time and limited overshoot.

While for a GFL the estimated angular speed $\widetilde{\omega}_g$ is obtained from a PLL, for a GFM, $\widetilde{\omega}_g$ is given as

$$\widetilde{\omega}_g = \omega_{vsm}. \tag{16}$$

After $\boldsymbol{i}_{\alpha\beta+}$ and $\boldsymbol{i}_{\alpha\beta-}$ are extracted, $\boldsymbol{i}_{dq+}$ and $\boldsymbol{i}_{dq-}$ are then obtained by the Park transformations, $P(\theta_{vsm})$ and $P(-\theta_{vsm})$.

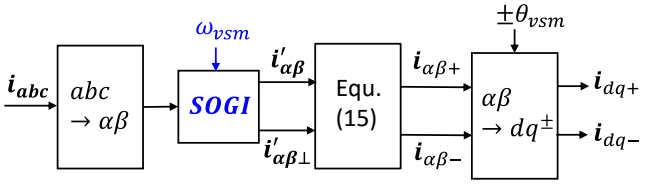

Figure 3. Sequence extraction using dual second order generalised integrator.

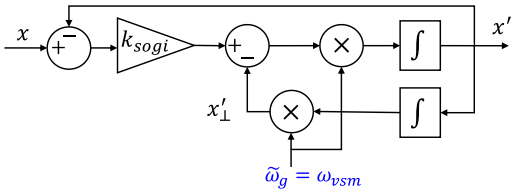

Figure 4. Adapted second order generalised integrator (SOGI).

C. Decoupled Double Synchronous Reference Frame (DDSRF)

The DDSRF in [17] is adapted for GFMs, and shown in Fig. 5. Based on the dq current signals in (11) and (12) in the two synchronous reference frames, the DDSRF principle decouples the sequence interactions by subtracting the interference of each sequence on the other.

Moving the terms with 2ω frequency to the left in (11) and (12), and then applying a low-pass filter (LPF) to both sides, it follows that

$$\overline{\boldsymbol{i}_{dq+}} = \frac{k\omega_{vsm}}{s+k\omega_{vsm}}\left(\boldsymbol{i}_{\alpha\beta}e^{-j\omega t} - \overline{\boldsymbol{i}_{dq-}}e^{-j2\omega t}\right), \tag{17}$$

$$\overline{\boldsymbol{i}_{dq-}} = \frac{k\omega_{vsm}}{s+k\omega_{vsm}}\left(\boldsymbol{i}_{\alpha\beta}e^{j\omega t} - \overline{\boldsymbol{i}_{dq+}}e^{j2\omega t}\right), \tag{18}$$

The filtered positive and negative current signals $\overline{\boldsymbol{i}_{dq+}}$ and $\overline{\boldsymbol{i}_{dq-}}$ can then be determined.

The LPF cut-off frequency is related to ω_{vsm}, and given as $\omega_f = k\omega_{vsm}$. Following [17], $k = 1/\sqrt{2}$, which offers a good tradeoff between dynamic overshoot and stabilisation speed. It will be demonstrated in Section V that the GFM under DSOGI with $k_{sogi} = \sqrt{2}$, and DDSFR with $\omega_f = 1/\sqrt{2}\omega_{vsm}$ achieves the same results.

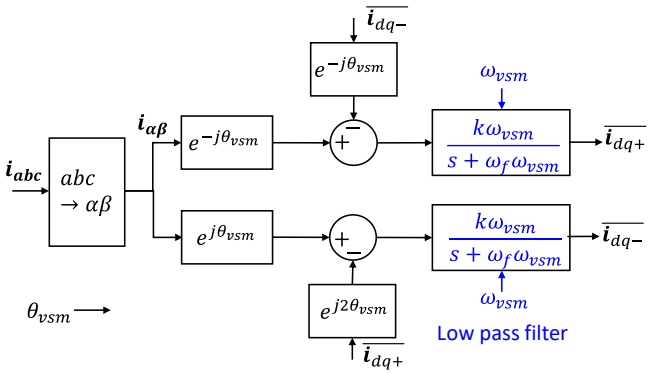

Figure 5. Sequence extraction using adapted decoupled double synchronous reference frame (DDSFR).

D. Notch Filter-Based Sequence Extraction

In [20] notch filter-based sequence extraction is used for GFMs, which is the same as the DDSRF method, excluding where the interference between each sequence is subtracted. Instead, notch filters directly filter the dq signals in the two synchronous reference frames, as shown in Fig. 6, where Q is the quality factor, and the resonant frequency is $\omega_o = 2\omega_{vsm}$.

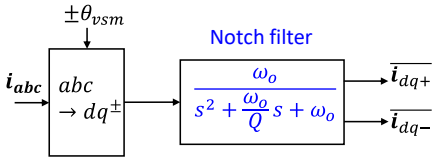

Figure 6. Sequence extraction using notch filters.

E. Sequence Extraction Comparison with Ideal Voltage Source

Before evaluating the above sequence extraction methods for GFMs, it is necessary to assess their performance for ideal voltage sources. A 100 ms voltage dip is applied, such that during the dip the positive and negative sequence voltages are given by $0.5\angle{-15}°$ and $0.4\angle{10}°$, respectively, relative to the balanced pre-fault voltage, $1\angle{0}°$. Given the testing with an ideal voltage source, ω_{vsm} is replaced by $2\pi f_b$ in the DSOGI, DDSRF and notch filter-based sequence extraction methods, while for the notch filter, $Q = 20$.

Fig. 7 shows the positive sequence voltage amplitude and angle obtained by the four sequence extraction methods. It can be seen that notch filter-based sequence extraction indicates the correct steady-state values, but large oscillations occur when the fault begins and clears (hence notch filter based method will not be demonstrated in Section V); delay cancellation achieves the correct results a quarter cycle after the fault, while DSOGI and DDSFR gives the correct results about one cycle later. It can thus be concluded that notch filter-based sequence extraction is not suitable, while the remaining approaches provide acceptable results, although the delay technique achieves the correct results the quickest.

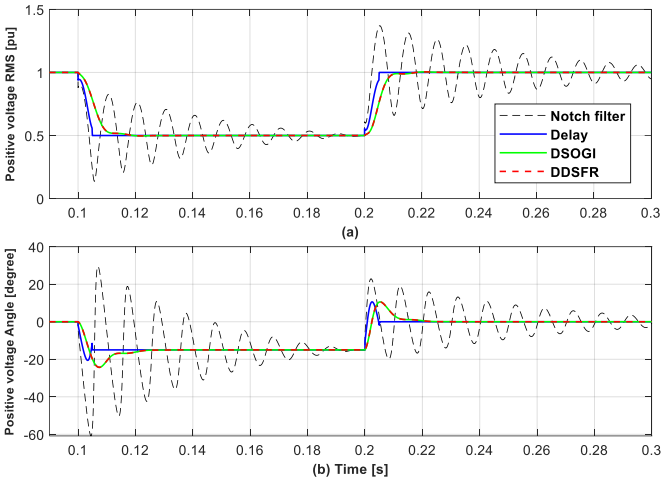

Figure 7. Positive sequence voltage amplitude and angle obtained by the four sequence extraction methods for an ideal voltage dip.

V. Case Studies

Six cases are now studied to evaluate GFM performance for different TVI and sequence extraction methods. The first two cases compare the proposed TVI against existing TVI current limiting control in [14][15]. Next, the three sequence extraction methods are compared, with, and without, the GFM current being limited, while the impacts of a switching delay are then shown for the three extraction methods. Finally, GFM dynamic stability is studied when using the measured current, or current reference, for the proposed TVI control in (1)-(7). All simulations are performed using the Modelica language [21], as implemented using Dymola software, whereby all modelling details are completely transparent and user-created models can be easily integrated.

A. GFM Performance for Proposed and Existing TVI Current Limiting Control

In Cases 1 and 2, the delay cancellation sequence extraction is implemented, as this method achieves the best performance in terms of harmonics, functionality, and stability relative to DSOGI and DDSFR, which will be shown in the next subsection. The converter switching delay is not implemented at this stage, as the focus here is the performance of the existing and proposed TVI current limiting control.

1) Symmetrical Short Circuit Fault

Case 1: A bolted symmetrical short circuit fault is applied at the PCC in Fig. 1. The equivalent grid resistance and reactance R_{eq} and L_{eq} are 0.02 pu and 0.2 pu based on the GFM MVA capacity. The active and reactive power setpoints of the GFM are 0.8 pu and 0 pu. The d-axis positive sequence voltage setpoint is 1 pu, and the q-axis positive sequence and d- and q-axis negative sequence voltage setpoints are zero. The maximum transient current limit is set at $I_{max} = 1.5$ pu [16]. The GFM parameters are summarized in Table I, based on parameters from [22]. Two scenarios are simulated:

(a) GFM is studied under the existing TVI current limiting control proposed in [14][15]. In [14][15], virtual reactance is not implemented. Hence, in order to compare against the proposed TVI control, virtual reactance is added (since virtual reactance can increase GFM transient stability). Based on the procedure in [15], the equivalent gain follows as $k_{pVI} = 1.51$ and $\sigma_{X/R} = 0.5$. Again similar to [14][15], current saturation limiting is also implemented, and TVI control is triggered when the current saturation limiting is active, i.e. $I_p^* \geq I_{max}$.

(b) GFM is studied under the proposed TVI current limiting control. In order to limit the current within 1.5 pu, and setting the triggering threshold current as $I_{nom} = 1.3$ pu and $\sigma_{X/R} = 0.5$, it is calculated that $k_{pVI} = 2.62$.

The simulation results for Case 1 are shown in Fig. 8, and Fig. 8(a) shows that under both TVI current limiting control schemes that the converter phase current is strictly limited within the maximum 1.5 pu, and maintains a sinusoidal waveform. Fig. 8(b) shows that the output voltage under the proposed TVI control is less distorted than that under the existing TVI control, since in the latter TVI control is only activated when the current saturation is active, which causes the GFM to lose its voltage source characteristics. Fig. 8(c) confirms this observation, as it is seen that I_p^* for the existing TVI exceeds the maximum limit I_{max}. However, for the proposed TVI no such current saturation limiters exist, as Fig. 8(c) shows that $I_p^* \leq I_{max}$. This is because the proposed TVI control is activated when $I_p^* \geq I_{nom}$ (where $I_{nom} < I_{max}$), instead of $I_p^* \geq I_{max}$. Hence, under the proposed TVI control, the GFM does not lose its voltage source characteristics.

Fig. 8(d) shows that for the existing TVI control, the GFM post-fault output voltage increases beyond the voltage setpoint of 1 pu (≈1.1 pu), and remains high for an extended period (≈250 ms) before recovering back to 1 pu, since with the GFM already in current limiting mode, the outer loop voltage integrator is still active. In contrast, for the proposed TVI control, the post-fault voltage quickly returns to 1 pu after exiting the current limiting mode, such that the overvoltage no longer occurs. Note that such overvoltage phenomenon can be mitigated by freezing the outer loop voltage integrator once the GFM is in current limiting mode.

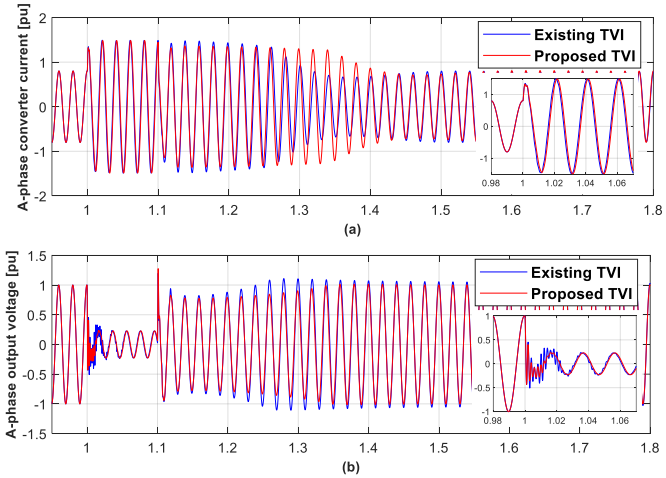

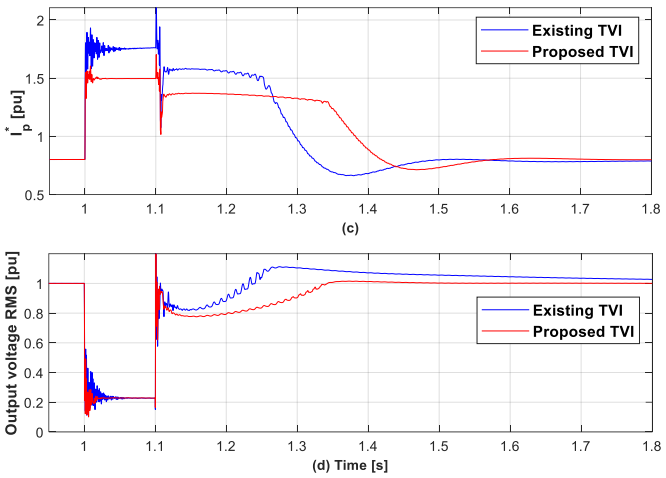

Figure 8. Case 1 for proposed and existing TVI current limiting control for a symmetrical fault. (a)(b) A-phase GFM converter current and output voltage (B- and C-phase are similar), (c) maximum (A, B or C) three-phase current reference amplitude, I_p^*, and (d) output voltage amplitude.

2) *Single-Line-to-Ground (SLG) Short Circuit Fault*

Case 2 is similar to Case 1, but for a SLG fault, with comparison results shown in Fig. 9. Fig. 9(a)(b) show that for both TVI current limiting control schemes that the phase currents are limited within 1.5 pu, and the phase currents are sinusoidal. Fig. 9(c)(d) show that the output phase voltages under the proposed TVI again are less distorted. Fig. 9(e) demonstrates that for both TVI methods that the GFM injects negative sequence current to suppress the negative sequence voltage. Fig. 9(f) shows that the GFM negative sequence output voltage for existing TVI control doesn't immediately return to zero once the fault is cleared, which leads to oscillations in the active power output, as seen in Fig. 9(g). As before, the outer loop voltage integrator is still active when the GFM is in current limiting mode during the fault period.

An isolated system with two GFMs for a line-to-line (LL) fault is also studied, with similar results to Case 2 obtained (not shown due to space limitations). It is thus concluded that the proposed TVI current limiting can strictly limit the GFM current and preserve GFM voltage source characteristics.

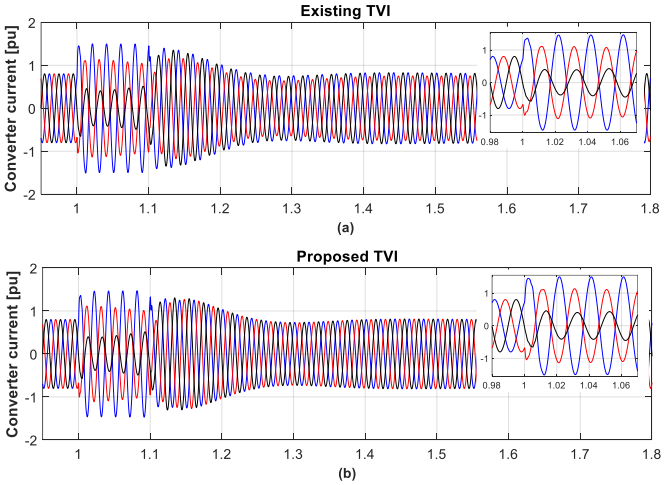

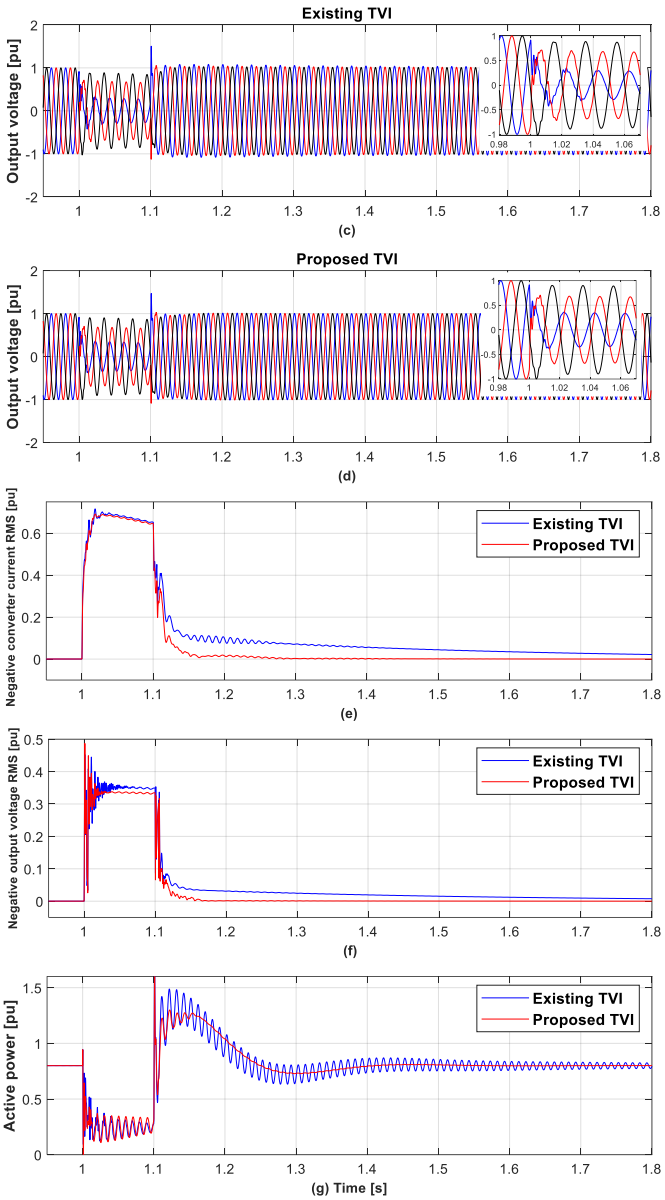

Figure 9. Case 2 for an asymmetrical fault. (a) and (b) Converter current under existing and proposed TVI current limiting control, (c) and (d) output voltage under proposed and existing TVI control, (e), (f) and (g) negative sequence output current amplitude, negative sequence output volage amplitude, and instaneous active power output.

B. *GFM Performance for Different Squence Extraction Methods*

1) *GFM In Current Unlimited Mode*

Case 3: The same as Case 2, but the bolted SLG fault is replaced by a less severe fault, i.e. adjusting one phase of the load from 0.11+j0.011 pu to 0.99+j0.11 pu, and the GFM active power setpoint is reduced from 0.8 pu to 0.6 pu. The GFM is simulated for the three sequence extraction methods, i.e. delay cancellation, DSOGI and DDSRF. The proposed TVI control is studied to limit the GFM current in Cases 3-5, as it exhibits better performance than the alternatives [14][15].

The results for Case 3 are shown in Fig. 10, and Fig. 10(a) shows that the converter current is less than 1.5 pu, i.e. in current unlimited mode. Hence, Fig. 10(b) shows that the GFM output voltages are balanced, with full controllability relative to the setpoints. Fig. 10 shows similar results for the DSOGI and DDSRF methods, indicating their equivalence for the chosen parameter settings, i.e. $k_{sogi} = \sqrt{2}$, $\tilde{\omega}_g = \omega_{vsm}$ for DSOGI, and $\omega_f = 1/\sqrt{2}\,\omega_{vsm}$ for DDSRF. However, for the delay cancellation method, the GFM current and output voltage indicate fewer oscillations immediately after the fault is applied and cleared, since it determines the positive and negative sequence voltage and current signals more quickly, as previously demonstrated in Section IV.E. Overall, the GFM achieves very similar performances for all three sequence extraction methods when not in current limited mode.

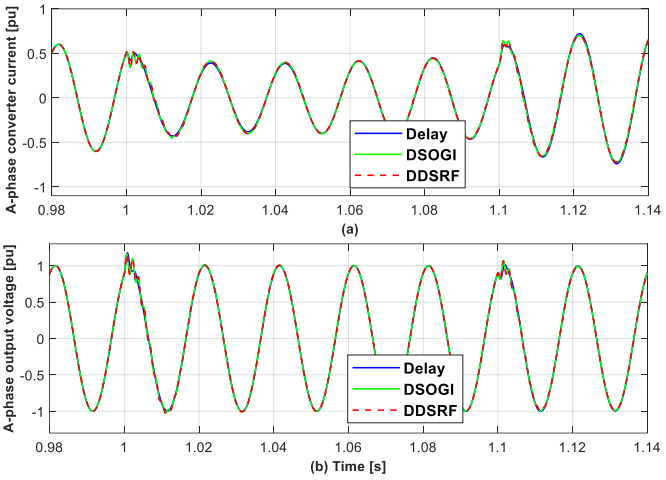

Figure 10. Case 3 under delay cancellation, DSOGI and DDSRF sequence extraction. (a) and (b) A-phase converter current and output voltage.

2) *GFM In Current Limiting Mode*

Case 4: The same as Case 3, but a bolted LL fault is now applied at the PCC. DDSRF sequence extraction results are not shown as they are the same as those for the DSOGI approach. The simulation results are shown in Fig. 11, and Fig. 11(a)(c) show that under the delay cancellation method the converter phase currents are limited ≤1.5 pu, while under the DSOGI method the B-phase current exceeds 1.5 pu, and it takes more than 1.5 cycles to return within 1.5 pu. Fig. 11(c)(d) show that the output voltage contains more harmonics under DSOGI in comparison to delay cancellation, similar to Case 3. As before, the differences in performance are due to the comparative execution speeds for both sequence extraction methods. Note that although increasing the gain k_{sogi} in the DSOGI method speeds up the extraction, and hence reduces the overcurrent amplitude and output voltage distortion (results not shown here), the converter current is still not strictly limited within 1.5 pu during the first cycle. Moreover, a larger k_{sogi} may introduce other stability issues.

It can thus be concluded that when the GFM is in current limiting mode that the delay cancellation sequence extraction method is applicable for GFM, while the DSOGI and DDSRF methods are not suitable since they are too slow to extract the sequence current signal, causing converter overcurrent and a distorted output voltage.

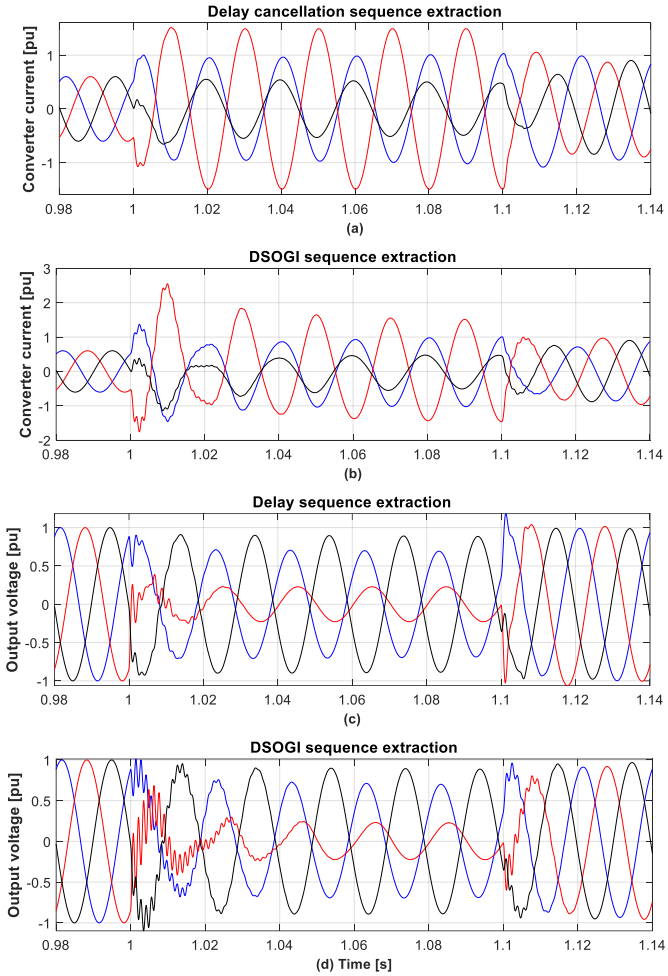

Figure 11. Case 4. (a) and (b) three phase converter currents; (c) and (d) three-phase output voltages for delay cancellation and DSOGI sequence extraction methods.

3) *Considering Switching Time Delay*

Case 5: Given that the time delay introduced by sequence extraction impacts GFM performance, converter switching delays are now investigated. The settings are the same as Case 4, but a switching delay of 250 μs is incorporated in the GFM model. The simulation results are shown in Fig. 12, and in comparison with Fig. 11(a)(c), Fig. 12(a)(c) show that with delay cancellation that a switching delay of 250 us has negligible impact on the GFM converter current and output voltage. However, when comparing against Fig. 11(b)(d), Fig. 12(b)(d) show that under DSOGI sequence extraction, when a switching delay of 250 μs is added that the phase current and output voltage are greatly distorted, with 800 Hz harmonics seen during the fault. Moreover, when a switching delay of 375 μs is simulated under the DSOGI method the GFM becomes unstable (results not shown here), while with delay cancellation the output voltages are similar to Fig. 11(c).

It can thus be concluded that the delay cancellation sequence extraction method is applicable for GFMs, while the DSOGI and DDSRF methods are not, when a large switching delay is considered.

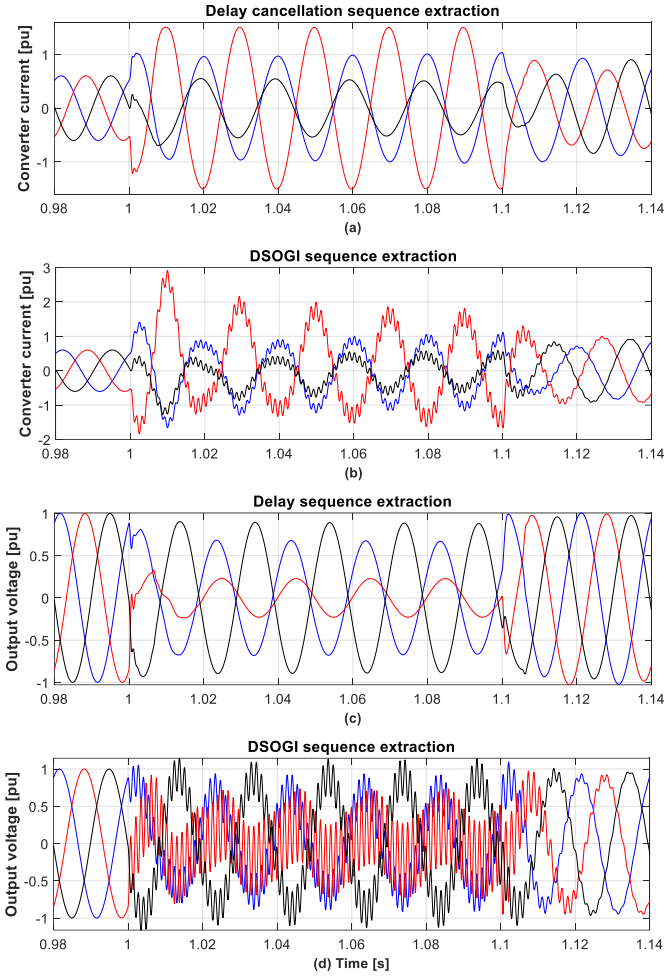

Figure 12. Case 5 with a switching delay of 250 μs. (a) and (b) 3-phase converter current; (c) and (d) 3-phase output voltage under delay cancellation and DSOGI sequence extraction methods.

C. *GFM Dynamics Comparison By Using Current Reference or Measured Current for Triggering the TVI Control*

Typically, the measured converter current is used to trigger and generate the virtual impedance in GFMs under balanced conditions. Under unbalanced conditions, since sequence extraction is needed, which introduces delays, it is of interest to consider whether the measured phase current or the existing current reference should be employed to trigger TVI control and generate the virtual impedance.

Case 6: Same as Case 5 (with delay cancellation sequence extraction method and proposed TVI current limiting control), except that the current reference signals for the TVI control in (1)-(7) are replaced by the relevant measured current. For example, $\boldsymbol{i}^*_{\boldsymbol{dq+}}$, $\boldsymbol{i}^*_{\boldsymbol{dq-}}$ and I^*_a, I^*_b, I^*_c are replaced by $\boldsymbol{i}_{\boldsymbol{dq+}}$, $\boldsymbol{i}_{\boldsymbol{dq-}}$ and I_a, I_b, I_c which are the measured signals from sequence extraction control. In addition, the switching delay is increased to 300 μs. The simulation results are shown in Fig. 13, and in comparison to Fig. 12(c), Fig. 13(a) shows that when using the current reference for TVI control, for a 300 μs switching delay, that the GFM output voltage is slightly more distorted, but still quickly returns to being sinusoidal. In contrast, Fig. 13(b) shows that when using the measured current for TVI control, large and persistence harmonics appear in the output voltage. The simulation results also show that when the delay is increased to 375 μs, when using the current reference for the TVI control, that the GFM remains stable, but when using the measured current for the TVI control, that the GFM becomes unstable as the oscillations increase (results not shown). The reason for the latter is again due to delays associated with sequence extraction when measuring the current signals.

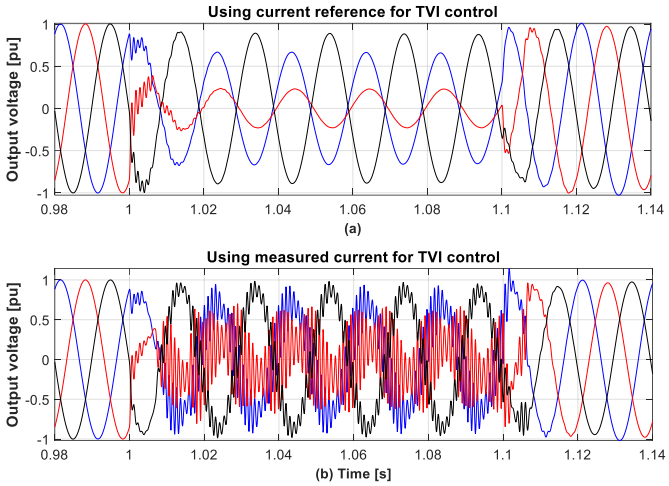

Figure 13. Case 6 with 300 μs switching delay. (a)(b) three-phase converter current using current reference or measured current for TVI control.

TABLE I. GRID-FORMING CONVERTER PARAMETERS

Parameters	**Values (pu)**
R_f, L_f, C_f, R_{tr}, L_{tr}	0.005, 0.15, 0.066, 0.005, 0.15
k_{pv}, k_{iv}, k_{pi}, k_{ii}	0.52, 1.16, 0.74, 1.19
I_{nom}, I_{max}	1.3, 1.5
m_p, m_q	0.02, 0.0001
ω_c, ω_{cq}	31.4 rad/s, 31.4 rad/s

VI. CONCLUSIONS

A TVI current limiting control scheme is proposed for GFMs which is applicable for both symmetrical and asymmetrical fault conditions. Simulation results demonstrate that the GFM converter current is strictly limited within the maximum limit, without requiring current saturation limiters, and GFM voltage source behavior is preserved. It is also demonstrated that using the measured current instead of the current reference to trigger TVI control, and generate the virtual impedance, may lead to unstable oscillations when a large switching delay is considered. Finally, GFM dynamic stability is studied for three well-known sequence extraction methods (i.e. delay cancellation, dual second order generalised integrator, and decoupled double synchronous reference frame). It is found that the performance differences are small

when the GFM is not in current limiting mode, but much more obvious when the GFM is in current limiting mode or switching delays are considered. Ongoing work by the authors aims to support the presented simulation results by performing theoretical analysis using frequency-lifting techniques such as dynamic phasor theory, and nonlinear large-signal stability analysis such as data-driven Lyapunov methods for GFMs under asymmetrical grid conditions.

ACKNOWLEDGMENT

The work has been supported by SEAI (Sustainable Energy Authority of Ireland) under RD&D Award 22/RDD/776.

REFERENCES

[1] J. Rocabert, A. Luna, F. Blaabjerg, and P. Rodriguez, "Control of power converters in AC microgrids," IEEE Transactions on Power Electronics, vol. 27, no. 11, pp. 4734-4749, 2012.

[2] M. Yu et al., "Instantaneous penetration level limits of non‐synchronous devices in the British power system," IET Renewable Power Generation, vol. 11, no. 8, pp. 1211-1217, 2017.

[3] X. Zhao, P. G. Thakurta, and D. Flynn, "Grid‐forming requirements based on stability assessment for 100% converter‐based Irish power system," IET Renewable Power Generation, vol. 16, no. 3, pp. 447-458, 2022.

[4] "H2020 MIGRATE Project, https://www.h2020-migrate.eu," ed, 2017.

[5] NGESO. "Expert group - Grid supporting fast fault current and associated control including virtual synchronous machine approaches," [Online] Available: https://www.nationalgrideso.com

[6] Infineon Technical report, 'AN2011-05 Industrial IGBT Modules Explanation of Technical Information', November 2015.

[7] N. Bottrell and T. C. Green, "Comparison of current-limiting strategies during fault ride-through of inverters to prevent latch-up and wind-up," IEEE Transactions on Power Electronics, vol. 29, no. 7, pp. 3786-3797, 2013.

[8] X. Zhao and D. Flynn, "Freezing grid-forming converter virtual angular speed to enhance transient stability under current reference limiting," in 2020 IEEE 21st Workshop on Control and Modeling for Power Electronics (COMPEL), 2020.

[9] A. D. Paquette and D. M. Divan, "Virtual impedance current limiting for inverters in microgrids with synchronous generators," IEEE Transactions on Industry Applications, vol. 51, no. 2, pp. 1630-1638, 2014.

[10] X. Zhao and D. Flynn, "Stability enhancement strategies for a 100% grid‐forming and grid‐following converter‐based Irish power system," IET Renewable Power Generation, vol. 16, no. 1, pp. 125-138, 2022.

[11] T. Qoria, F. Gruson, F. Colas, X. Kestelyn, and X. Guillaud, "Current limiting algorithms and transient stability analysis of grid-forming VSCs," Electric Power Systems Research, vol. 189, p. 106726, 2020.

[12] Q. Taoufik, H. Wu, X. Wang, and I. Colak, "Variable virtual impedance-based overcurrent protection for grid-forming inverters: small-signal, large-signal analysis and improvement," IEEE Transactions on Smart Grid, vol. 14, no. 5, pp. 3324-3336, Sept. 2023.

[13] T. Qoria, F. Gruson, F. Colas, G. Denis, T. Prevost, and X. Guillaud, "Critical clearing time determination and enhancement of grid-forming converters embedding virtual impedance as current limitation algorithm," IEEE Journal of Emerging and Selected Topics in Power Electronics, vol. 8, no. 2, pp. 1050-1061, 2019.

[14] S. F. Zarei, H. Mokhtari, M. A. Ghasemi, and F. Blaabjerg, "Reinforcing fault ride through capability of grid forming voltage source converters using an enhanced voltage control scheme," IEEE Transactions on Power Delivery, vol. 34, no. 5, pp. 1827-1842, 2018.

[15] A. H. Jafariazad, S. A. Taher, Z. D. Arani, M. H. Karimi, and J. M. Guerrero, "Adaptive supplementary control of VSG based on virtual impedance for current limiting in grid-connected and islanded microgrids," IEEE Transactions on Smart Grid, 2023. doi: 10.1109/TSG.2023.3274628.

[16] R. Rosso, S. Engelken, and M. Liserre, "On the implementation of an FRT strategy for grid-forming converters under symmetrical and asymmetrical grid faults," IEEE Transactions on Industry Applications, vol. 57, no. 5, pp. 4385-4397, 2021.

[17] P. Rodríguez, J. Pou, J. Bergas, J. I. Candela, R. P. Burgos, and D. Boroyevich, "Decoupled double synchronous reference frame PLL for power converters control," IEEE Transactions on Power Electronics, vol. 22, no. 2, pp. 584-592, 2007.

[18] Y. Zhou, P. Bauer, J. A. Ferreira, and J. Pierik, "Operation of grid-connected DFIG under unbalanced grid voltage condition," IEEE Transactions on Energy Conversion, vol. 24, no. 1, pp. 240-246, 2009.

[19] P. Rodriguez, R. Teodorescu, I. Candela, A. V. Timbus, M. Liserre, and F. Blaabjerg, "New positive-sequence voltage detector for grid synchronization of power converters under faulty grid conditions," in 2006 37th IEEE Power Electronics Specialists Conference, 2006.

[20] B. Mahamedi, M. Eskandari, J. E. Fletcher, and J. Zhu, "Sequence-based control strategy with current limiting for the fault ride-through of inverter-interfaced distributed generators," IEEE Transactions on Sustainable Energy, vol. 11, no. 1, pp. 165-174, 2018.

[21] P. Fritzson, Principles of object-oriented modeling and simulation with Modelica 3.3: a cyber-physical approach. John Wiley & Sons, 2014.

[22] T. Qoria, F. Gruson, F. Colas, X. Guillaud, M.-S. Debry, and T. Prevost, "Tuning of cascaded controllers for robust grid-forming voltage source converter," in 2018 Power Systems Computation Conference (PSCC), 2018.